

# Analysis and Design of a Repetitive Predictive-PID Controller for PWM Inverters

C. Rech, H. Pinheiro, H. A. Gründling, H. L. Hey, J. R. Pinheiro

Federal University of Santa Maria

UFSM – CT – DELC – NUPEDEE

ZIP CODE: 97105-900 – Santa Maria, RS – Brazil

E-mail: cassiano@nupedeec.ufsm.br, renes@ctlab.ufsm.br

**Abstract** — This paper presents a predictive PID controller including a feedforward control and a repetitive controller for UPS applications. This digital control scheme can minimize periodic distortions resulted from nonlinear cyclic loads. Design procedure and stability analysis of the control scheme are discussed. Simulation and experimental results for a single-phase PWM inverter (110 V<sub>RMS</sub>, 1 kVA) controlled by a low cost microcontroller are presented to demonstrate the performance of the proposed control approach under periodic load disturbances.

## I. INTRODUCTION

Due to widespread use of the microcomputer-based systems in several applications, the demand of single-phase uninterruptible power systems to supply critical loads at low power (500 VA - 5 kVA) is increasing. On the other hand, with the fast development of the low cost microcontrollers, engineers and researchers have been using more sophisticated digital control techniques to improve the performance of the uninterruptible power supplies (UPS) [1]-[2]. As result, compact systems of low cost, good performance and great reliability have been obtained.

In this application, the purpose of a digital control scheme is to generate a PWM (Pulse Width Modulation) pattern to produce the sinusoidal output voltage of the UPS system with low total harmonic distortion (THD) even under both transient or load disturbances. Among the digital control techniques, the digital PID (proportional-integral-derivative) controller has been used in many industrial control systems. The main reason for this is its simplicity, along with the flexibility of a digital controller. The disadvantage of this controller is that the delay time caused by A/D conversion and computation time of the microprocessor reduces the maximum available pulse width. Hence, this limitation can result in output voltage waveform distortions. One method for overcoming this time delay was developed [3] and the resulting controller is called a PID predictor controller [3]-[4]. However, by using this controller in PWM inverters, the output voltage waveform may present a high THD specially when the load is nonlinear such as ac phase-controlled loads and rectifier loads.

Repetitive control theory [5] provides an alternative to minimize periodic errors occurred in a dynamic system. The repetitive control improves the accuracy of the steady state response of a control system when the reference input signal and disturbances are periodic, consisting of harmonic

components of a common fundamental frequency. Several repetitive control schemes have been developed and applied to various industrial applications [6]-[7]. Besides, the repetitive control technique has been applied to minimize periodic errors which can appear in single-phase PWM inverters [8]-[10].

In this paper is proposed a predictive PID controller including a feedforward control and a repetitive controller for UPS applications. This digital control technique can minimize periodic distortions resulted from nonlinear cyclic loads, even in the presence of unmodeled dynamics. Moreover, due to error prediction, it is possible to implement this controller on a low cost microcontroller.

This paper is organized as follows. Section II describes the plant model. The structure, design procedure and stability analysis of the predictive PID-feedforward controller with a repetitive controller for a single-phase PWM inverter are presented in Section III. Section IV presents simulation results with nonlinear loads and Section V shows experimental results obtained for linear and nonlinear loads based on a microcontroller-controlled system.

## II. PLANT MODEL

Fig. 1 shows the single-phase PWM inverter, where the full-bridge inverter, LC filter, and resistive load  $R$  are considered as the plant to be controlled. A triac connected in series with a resistive load or a full-bridge rectifier with RC filter can be used to evaluate the performance of the system with nonlinear loads. As a matter of fact, due to diversity of loads, it is not possible to formulate a general model to cover every kind of load. However, we can define a nominal load to derive its linear model and consider load variations and model uncertainties as a load disturbance.

The system transfer function of the Fig. 1 is given by

$$\frac{Y(s)}{U(s)} = G(s) = \frac{\omega_n^2}{s^2 + 2\zeta\omega_n s + \omega_n^2} \quad (1)$$

where  $\omega_n = 1/\sqrt{LC}$ ,  $\zeta = 1/(2RC\omega_n)$ ,  $Y(s)$  is the Laplace transform of the system output  $y(t) = v_c(t)$  and  $U(s)$  is the Laplace transform of the system input  $u(t) = v_{in}(t)$ .

In the following analysis the power switches are turned on and off once during each sampling interval  $T$ , such that  $v_{in}(t)$  is a voltage pulse of magnitude  $V_B$ , 0 or  $-V_B$  and width  $\Delta T$ .

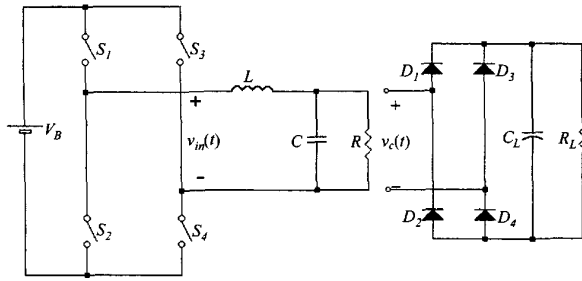


Fig. 1 – PWM inverter system.

From (1), a discrete transfer function can be obtained using a zero-order hold with an appropriate sampling time  $T$  [11],

$$G(z) = \frac{b_1 z + b_2}{z^2 + a_1 z + a_2} \quad (2)$$

### III. PREDICTIVE PID-FEEDFORWARD CONTROLLER WITH REPETITIVE CONTROLLER

#### A. Structure of the Controller

The classic PID controller, shown in Fig. 2, has been used in many industrial control systems. The main reasons are its simple structure, which can be easily understood and implemented in the practice, and its excellent flexibility made possible by the adjustment of the coefficients  $K_P$ ,  $K_I$  e  $K_D$ .

The equation for the controller in Fig. 2 is

$$u_{PID}(t) = K_P e(t) + K_I \int e(t) dt + K_D \frac{de(t)}{dt} \quad (3)$$

For a microcontroller implementation, (3) becomes

$$u_{PID}(k) = K_P e(k) + K_I T \sum_{n=1}^k e(n) + \frac{K_D}{T} [e(k) - e(k-1)] \quad (4)$$

According to (4), the control variable  $u_{PID}(k)$  depends upon the present value of the error signal  $e(k)$  as well as its previous values. If the required computation time to implement  $u_{PID}(k)$  is not small, benefits may be reached in predicting the value of  $e(k)$  at time  $t = (k-1)T$ , and then computing  $u_{PID}(k)$  from (4). However, errors are introduced into the system since the predicted value of  $e(k)$  is used rather than the true one [4].

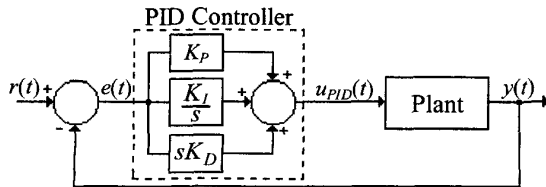


Fig. 2 – Classic PID controller.

Aylor, Ramey and Cook [3] used the simple linear prediction algorithm, given by:

$$e(k) = e(k-1) + [e(k-1) - e(k-2)] \quad (5)$$

where the error signal is predicted according to their last two measured values.

Using (5) to predict  $e(k)$  in (4), the predictive PID controller equation becomes

$$u_{PID}(k) = [2K_P + 2K_I T + K_D / T] e(k-1) - [K_P + K_I T + K_D / T] e(k-2) + [K_I T] \sum_{n=1}^{k-1} e(n) \quad (6)$$

To minimize the tracking error for linear and nonlinear cyclic loads, a feedforward control and a repetitive controller are added to predictive PID controller, as shown in Fig. 3.

Then, the control law  $u_P(k)$  becomes:

$$u_P(k) = u_{PID}(k) + u_{RP}(k) + r(k) \quad (7)$$

In a similar way as presented in [9], the repetitive control law can be written as:

$$u_{RP}(k) = c_1 e(k+N-n) + c_2 \sum_{i=1}^{\infty} e(k+N-i.n) \quad (8)$$

where  $e(k)$  is the tracking error,  $c_1$  and  $c_2$  are the gains of the repetitive controller,  $N$  is the time advance step size and  $n$  is the number of samples in a period of reference voltage.

Due to inclusion of the repetitive controller in the control law, it is possible to eliminate the integral action from the PID controller, therefore reducing the computational effort for the controller implementation without degrade the performance of the system. By removing the integration from the predictive PID controller, (6) becomes,

$$u_{PID}(k) = K_1 e(k-1) + K_2 e(k-2) \quad (9)$$

where

$$\begin{aligned} K_1 &= 2K_P + K_D / T \\ K_2 &= -K_P - K_D / T \end{aligned} \quad (10)$$

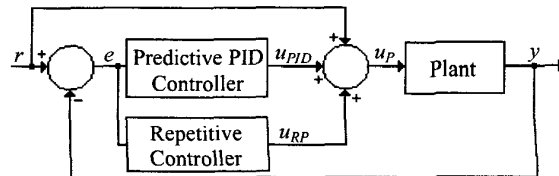


Fig. 3 – Simplified block diagram of the proposed control system.

### B. Controller Design

Fig. 4 shows the block diagram of the feedback system, using the predictive PID-feedforward controller. The closed-loop transfer function of the system shown in Fig. 4 is given by

$$G_{PID}(z) = \frac{b_1 z^3 + (b_1 K_1 + b_2) z^2 + (b_1 K_2 + b_2 K_1) z + b_2 K_2}{z^4 + a_1 z^3 + (a_2 + b_1 K_1) z^2 + (b_1 K_2 + b_2 K_1) z + b_2 K_2} \quad (11)$$

From (11), it is observed that the characteristic equation of the feedback system is a fourth-order polynomial. However, for this case, it was verified that the closed-loop system has two poles that are dominant. Then, the characteristic equation can be represented by

$$P_c(z) = (z - p_1)(z - p_2)(z - p_D)(z - \bar{p}_D) \quad (12)$$

where  $p_D$  and  $\bar{p}_D$  are dominant poles of the closed-loop system in the  $z$  domain and,  $p_1$  and  $p_2$  are the other two poles of the feedback system. The location of the dominant poles of the closed-loop system in the  $s$  domain is given by:

$$S_{1,2} = -\zeta_c \omega_c \pm j \omega_c \sqrt{1 - \zeta_c^2} \quad (13)$$

where  $\omega_c$  and  $\zeta_c$  are, respectively, the natural frequency and damping ratio of the desired closed-loop system. Consequently, the location of the dominant poles in the discrete domain ( $z$  domain) is given by:

$$\begin{aligned} p_D &= e^{S_1 T} \\ \bar{p}_D &= e^{S_2 T} \end{aligned} \quad (14)$$

Therefore, by using the predictive PID-feedforward controller, which has two parameters ( $K_1$  and  $K_2$ ), it is possible to place the two dominant poles of the closed-loop system, such that the feedback system satisfies the desired specifications.

For example, we choose a damping ratio  $\zeta_c = 0.4$  and a natural frequency ( $\omega_c$ ) 10% greater than the natural frequency of the plant. Then, the parameters of predictive PID controller, by using the denominator of (11) and (12)-(14), are given by

$$\begin{aligned} K_1 &= 0.1033 \\ K_2 &= -0.2523 \end{aligned}$$

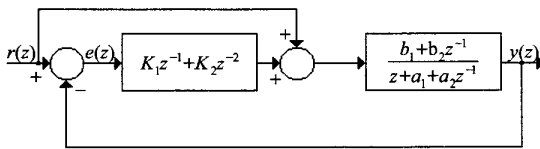


Fig. 4 – Block diagram of the closed-loop system using the predictive PID-feedforward controller.

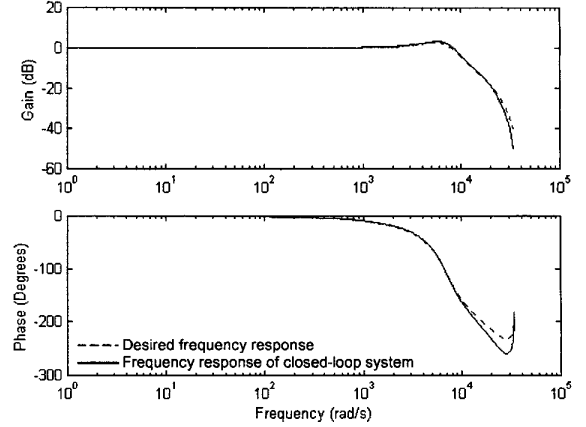


Fig. 5 – Frequency response of the system.

In Fig. 5 is shown the small influence of the poles  $p_1$  and  $p_2$  in the frequency response of the closed-loop system, verifying that the frequency response of the closed-loop system is similar to the desired frequency response.

The repetitive controller gains used in all simulations and experiments are  $c_1 = 0.02$  and  $c_2 = 0.20$ . With these gains, the feedback system has a good steady-state response for any resistive load and a fast convergence of the output error for nonlinear cyclic loads.

### C. Stability Analysis

The closed-loop system with the predictive PID-feedforward controller is stable if all roots of the denominator of (11) lie within the unit circle.

By simulation, various values of  $K_1$  and  $K_2$  were found for different values of load resistance  $R$ , which caused one or more roots of the denominator of (11) to lie on the unit circle (the stability boundary) with all other roots inside the circle. In this way, the family of curves shown in Fig. 6 was generated, where each curve represents the limiting values of  $K_1$  and  $K_2$  for a selected load resistance  $R$ .

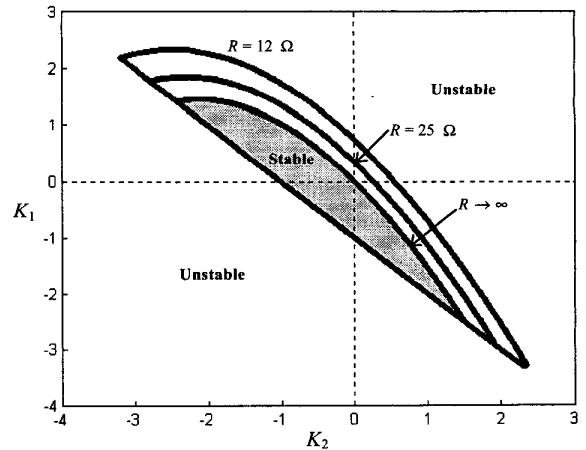


Fig. 6 – Limiting values of  $K_1$  versus  $K_2$  for stable operation ( $L = 1$  mH,  $C = 25$   $\mu$ F,  $T = 92.6$   $\mu$ s).

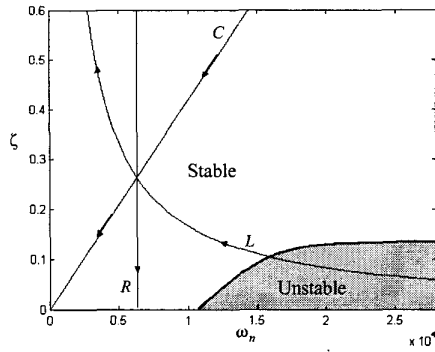


Fig. 7 – Stability region of the predictive PID-feedforward controller in  $\zeta - \omega_n$  plane (Nominal values:  $R = 12 \Omega$ ,  $C = 25 \mu\text{F}$ ,  $L = 1 \text{ mH}$ ).

In Fig. 7 are presented the trajectories of the plant parameters in the  $\zeta - \omega_n$  plane. For a given trajectory, one parameter varies along the trajectory and the other two parameters are held constant with their nominal values. This figure indicates that the predictive PID-feedforward controller, by using  $K_1 = 0.1033$  and  $K_2 = -0.2523$ , is stable for any value of  $\omega_n$ , smaller than 10500 rad/s.

With the inclusion of the repetitive control, the transfer function  $E(z)/R(z)$  of the system shown in Fig. 3, by using (2) and after  $z$ -transforming of (7)–(9), is given by

$$\frac{E(z)}{R(z)} = \frac{(1-G_{PID}(z))(1-z^{-n})}{1-z^{-n}H_{PID}(z)} \quad (15)$$

where the  $z$ -transform of the output error is  $E(z)$ ,  $R(z)$  is the transformed reference input, and

$$H_{PID}(z) = 1 - \frac{z^{N+2}}{z^2 + K_1 z + K_2} (c_1 + c_2 - c_1 z^{-n}) G_{PID}(z) \quad (16)$$

Assuming that (11) is stable, then the stability of the system is determined by the repetitive control. From (15), it is possible to demonstrate that the sufficient condition [9] for the stability is

$$|H_{PID}(j\omega)| \leq 1 \quad (17)$$

where  $\omega = 2\pi m f$  ( $m = 0, 1, 2, \dots, n/2$ ).

#### IV. SIMULATION RESULTS

Table I gives the parameters of the single-phase full-bridge PWM inverter system used in digital computer simulation with MATLAB<sup>®</sup> to verify the performance of the proposed control scheme.

In Fig. 8 is presented the output voltage  $v_c(t)$  and load current  $i_L(t)$  waveforms for rated resistive load with phase commutated at angle of  $72^\circ$ . Fig. 9 shows the output voltage  $v_c(t)$  and load current  $i_L(t)$  waveforms for the same nonlinear cyclic load including an unmodeled zero at  $-80000 \text{ rad/s}$ . This

TABLE I

PARAMETERS OF PWM INVERTER.

Filter inductance	$L = 1 \text{ mH}$
Filter capacitance	$C = 25 \mu\text{F}$
DC input voltage	$V_B = 200 \text{ V}$
Reference voltage	$r = 110 \text{ V}_{\text{RMS}}, f = 60 \text{ Hz}$
Linear load	$R = 12 \Omega$
Nonlinear load	$R_L = 25 \Omega$
	$C_L = 330 \mu\text{F}$
Sampling frequency	$f_s = 10800 \text{ Hz}$
Sampling time	$T = 92.6 \mu\text{s}$

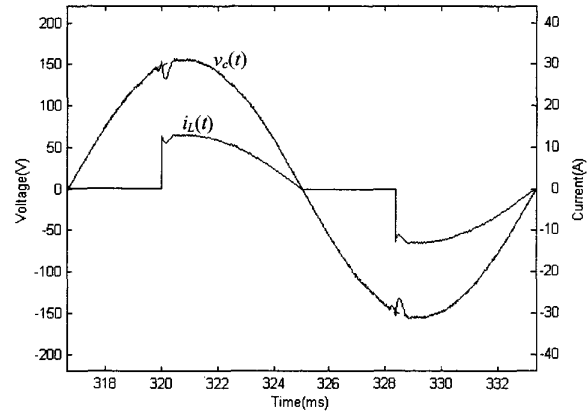


Fig. 8 – Output voltage  $v_c(t)$  and load current  $i_L(t)$  waveforms for rated resistive load with phase commutated at angle of  $72^\circ$ .

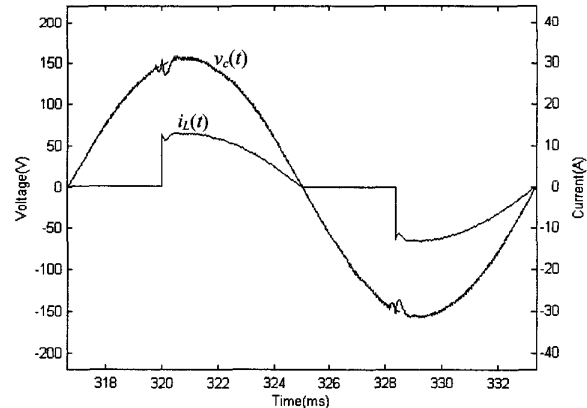


Fig. 9 – Output voltage  $v_c(t)$  and load current  $i_L(t)$  waveforms for rated resistive load with phase commutated at angle of  $72^\circ$  with the inclusion of a unmodeled stable zero at  $-80000 \text{ rad/s}$ .

unmodeled stable zero could be physically represented by an unmodeled equivalent series resistance (ESR) of  $0.5 \Omega$  of the filter capacitor. Unlike OSAP controller [10], it is observed that the proposed controller presents a good performance even with the inclusion of unmodeled dynamics.

Fig. 10 presents the response of PID-feedforward controller with repetitive controller for a rectifier load. In Fig. 11 is shown the output voltage and load current waveforms under a step load change from no load to full load, demonstrating the good transient response of this controller for a step load change.

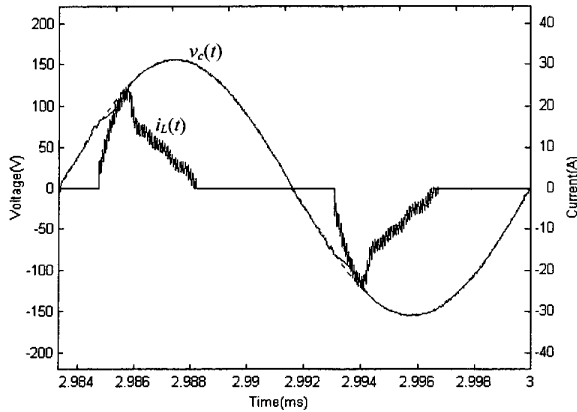


Fig. 10 – Output voltage  $v_c(t)$  and load current  $i_L(t)$  waveforms for a rectifier-RC load.

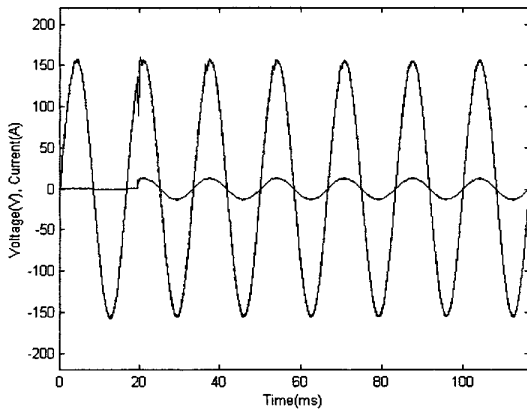


Fig. 11 – Output voltage and load current waveforms under a step load change from no load to full load.

## V. EXPERIMENTAL RESULTS

An IGBT prototype of the single-phase PWM inverter has been built in laboratory to verify the performance of the predictive PID-feedforward controller with repetitive controller. The component values of the inverter system and rectifier-RC load are given in Table I.

The simplified block diagram of the experimental setup is shown in Fig. 12. The controller has been implemented using an eight bits wide data word microcontroller (PIC17C756 of Microchip Technology Inc.). It has an embedded 10 bits A/D converter and a PWM signal generator. These features reduce significantly the PWM inverter control circuitry without penalizing the cost.

Fig. 13 shows the output voltage  $v_c(t)$  (THD = 1.49%) and load current  $i_L(t)$  waveforms for nominal resistive load (12  $\Omega$ /1 kVA). Fig. 14 presents the reference voltage  $r(t)$ , which is generated by the microcontroller and a D/A converter (DAC0800), and output voltage  $v_c(t)$  waveforms for nominal resistive load, demonstrating the tracking capability of this controller.

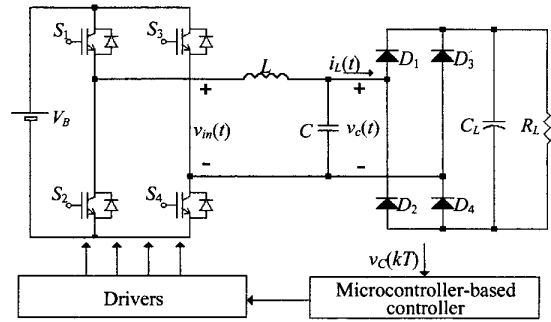


Fig. 12 – Block diagram of the experimental setup.

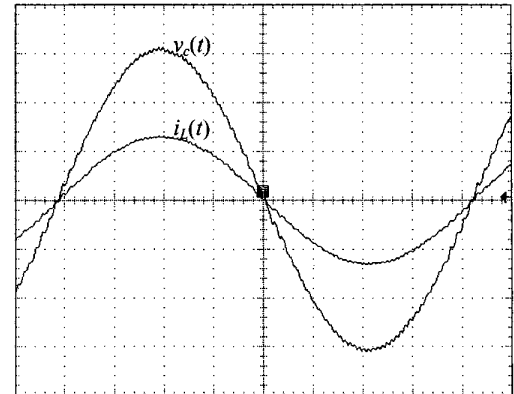


Fig. 13 – Output voltage (50 V/div) and load current (10 A/div) for nominal resistive load. Time scale 2 ms/div.

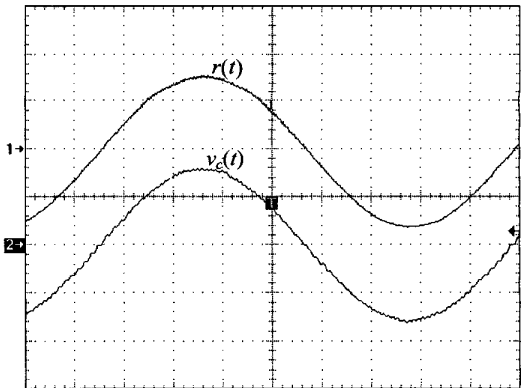


Fig. 14 – Reference voltage (5 V/div) and output voltage (100 V/div) for nominal resistive load. Time scale 2 ms/div.

To check the response of the proposed control scheme for a nonlinear load, the resistive load was replaced by a rectifier with RC filter, as shown in Fig. 12. Fig. 15 shows the output voltage  $v_c(t)$  (THD = 2.41%) and load current  $i_L(t)$  waveforms for a rectifier-RC load. Fig. 16 presents the reference voltage  $r(t)$  and output voltage  $v_c(t)$  waveforms for the same rectifier-RC load, to demonstrate the tracking capability of this controller for nonlinear loads. Fig. 17 shows the output voltage  $v_c(t)$  and the input filter voltage  $v_{in}(t)$  waveforms for this nonlinear load.

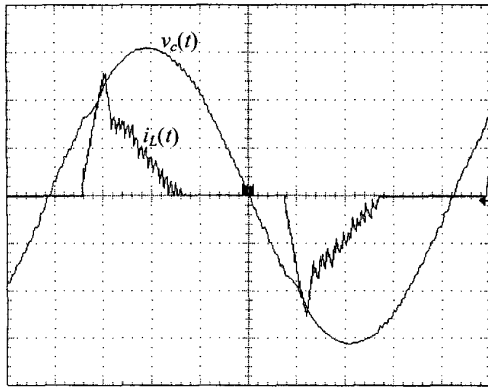


Fig. 15 – Output voltage (50 V/div) and load current (10 A/div) for a rectifier-RC load. Time scale 2 ms/div.

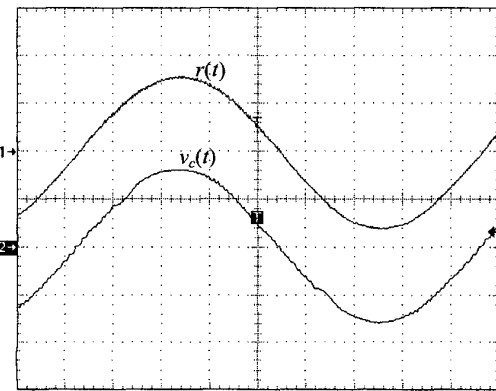


Fig. 16 – Reference voltage (5 V/div) and output voltage (100 V/div) for a rectifier-RC load. Time scale 2 ms/div.

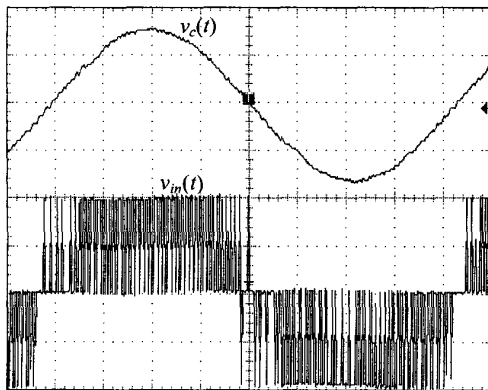


Fig. 17 – Output voltage (100V/div) and filter input voltage (100V/div) for a rectifier-RC load. Time scale 2 ms/div.

## VI. CONCLUSIONS

This paper describes a predictive PID controller including a feedforward and a repetitive control actions for UPS applications. Simulation results show that the proposed control scheme can minimize distortions resulted by nonlinear cyclic loads and unmodeled dynamics. Stability analysis accomplished in this paper demonstrate that the closed-loop system is stable for any resistive load. Besides, the use of a predictive controller makes possible the implementation of the control law on a low cost microcontroller at low and medium switching frequencies. Even with the limitations of the processing speed and fixed-point routines, this control algorithm presents a good performance. Furthermore, it has been experimentally demonstrated the good performance of the proposed controller under different load conditions.

## REFERENCES

- [1] A. Kawamura, T. Haneyoshi and R. G. Hoft, "Deadbeat controlled PWM inverter with parameter estimation using only voltage sensor", *IEEE Trans. on Power Electronics*, v. 3, n. 2, pp. 118-125, Apr. 1988.
- [2] S. L. Jung and Y. Y. Tzou, "Discrete sliding-mode control of a PWM inverter for sinusoidal output waveform synthesis with optimal sliding curve", *IEEE Trans. on Power Electronics*, v. 11, n. 4, pp. 567-577, Jul. 1996.
- [3] J. H. Aylor, R. L. Ramey and G. Cook, "Design and application of a microprocessor PID predictor controller", *IEEE Trans. on Ind. Electronics and Control Instrumentation*, v. 27, n. 3, pp. 133-137, Aug. 1980.
- [4] C. L. Phillips and J. M. Parr, "Robust design of a digital PID predictor Controller", *IEEE Trans. on Industrial Electronics*, v. 31, n. 4, pp. 328-332, Nov. 1984.
- [5] S. Hara, Y. Yamamoto, T. Omata and M. Nakano, "Repetitive control system: A new type servo system for periodic exogenous signals", *IEEE Trans. on Automatic Control*, v. 33, n. 7, pp. 659-667, Jul. 1988.
- [6] T. Inoue, "Practical repetitive control system design", in *Proceedings of the 29<sup>th</sup> Conference on Decision and Control*, Honolulu, Hawaii, pp. 1673-1678, Dec. 1990.
- [7] M. Ikeda and M. Takano, "Repetitive control for systems with nonzero relative degree", in *Proceedings of the 29<sup>th</sup> Conference on Decision and Control*, Honolulu, Hawaii, pp. 1667-1672, Dec. 1990.
- [8] Y. Nishida and T. Haneyoshi, "Predictive instantaneous value controlled PWM inverter for UPS", *IEEE Power Electronics Specialists Conference*, v. 2, pp. 776-783, 1992.
- [9] T. Haneyoshi, A. Kawamura and R. G. Hoft, "Waveform compensation of PWM inverter with cyclic fluctuating loads", *IEEE Trans. on Industry Applications*, v. 24, n. 4, pp. 582-588, Jul./Aug. 1988.
- [10] C. Rech, H. A. Gründling and J. R. Pinheiro, "A modified discrete control law for UPS Applications", in *IEEE Power Electronics Specialists Conference Rec.*, v. 3, pp. 1476-1481, 2000.
- [11] K. J. Astrom and B. Wittenmark, *Computer-Controlled Systems: Theory and Design*. Upper Saddle River, NJ: Prentice-Hall, 1997.